Fermi National Accelerator Laboratory

FERMILAB-Pub-92/196-T

Top Search in Multijet Signals

F.A. Berends, J.B. Tausk*
Instituut-Lorentz, University of Leiden,
P.O.B. 9506, 2300 RA Leiden, The Netherlands.

and

W.T. Giele†
Fermi National Accelerator Laboratory, P.O. Box 500,
Batavia, IL 60510, U.S.A.

August 25, 1992

Abstract

We investigate the possibilities of finding the top quark at the FNAL Tevatron $p\bar{p}$ collider ($\sqrt{s} = 1.8$ TeV) in the lepton plus multijet signal. The theoretical uncertainties in the normalization of the top production cross section and background signals make it important to look for the top in a final state where the top mass is reconstructible from the final state. The $W + 4$ jet final state offers a simple and direct way to reconstruct the top mass through final state invariant masses. It is shown that from a theoretical viewpoint the top is easily recovered from this $W + 4$ jet cross section. The only limitation comes from the experimental ability to correctly reconstruct the invariant masses which might contain multiple jets.

*Research supported by the Stichting FOM
†SSC fellow.

Operated by Universities Research Association Inc. under contract with the United States Department of Energy

1 Introduction

The present direct top mass limit of $m_{top} > 91$ GeV from the CDF collaboration used an integrated luminosity of roughly 5 pb^{-1} [1]. Based on indirect constraints obtained from the standard model using a combination of measurements, in particular the combined LEP data [2], the top mass is likely to be in the range $m_{top} = 132\ ^{+45}_{-50}$ GeV. This means the current collider run at Fermilab, yielding at least 25 pb^{-1} of integrated luminosity, should produce enough events to establish the existence of the top quark.

Given the above top quark mass limit and expected top mass, the dominant production process of top quarks is direct $t\bar{t}$ production. The top quark will subsequently decay into a b quark and a W boson, resulting in the following signatures which can be used in the top search

$$p\bar{p} \rightarrow t\bar{t} \rightarrow b\bar{b}\ W^+W^- \rightarrow b\bar{b}\ jj\ jj \tag{1.1}$$

$$p\bar{p} \rightarrow t\bar{t} \rightarrow b\bar{b}\ W^+W^- \rightarrow b\bar{b}\ l\nu\ jj \tag{1.2}$$

$$p\bar{p} \rightarrow t\bar{t} \rightarrow b\bar{b}\ W^+W^- \rightarrow b\bar{b}\ l\nu\ l'\nu' \tag{1.3}$$

where j denotes the jet originating from the hadronic W decays. Other authors have investigated single top quark production [3], but that does not yield promising results for the Fermilab collider. We shall denote the various channels by the number of hard isolated charged leptons in the event.

The highest event rate is given by the zero lepton process (1.1) with its relative branching fraction of $\left(\frac{2}{3}\right) \times \left(\frac{2}{3}\right)$. Unfortunately this multijet final state suffers from a huge QCD background and seems only usable when one of the b-jets can be tagged. Even then the background is still much larger than the signal. We refer to ref. [4, 5] for a more detailed discussion.

The single lepton channel (1.2) has a smaller event rate with a relative weight of $2 \times \left(\frac{2}{9}\right) \times \left(\frac{2}{3}\right)$ (counting both electron/positron and muon/antimuon final states). However the QCD background is strongly reduced by the presence of the isolated lepton, making it possible to get a signal over background ratio of order one. The main purpose of the present paper is to study this one lepton signature and its background in more detail than in ref. [6]. In particular it will be shown how specific distributions can greatly improve the extraction of the signal. Depending on the mass difference of the top and the W vector boson the signal (1.2) can show up as one lepton with 2, 3 or 4 jets. With an increasing number of jets the calculation of the exact background cross section

$$p\bar{p} \rightarrow W + n \text{ jets} \tag{1.4}$$

becomes more and more involved. The $n = 3$ case was considered in refs. [7, 8] and the $n = 4$ in ref. [6]. Some discussion of top signal versus background was given in ref. [6] and also in ref. [9], but in the latter a shower Monte Carlo was used to estimate (1.4) and not the exact evaluation. All the results for the single lepton channel in this paper refer to the sum of e^+ and e^- signals. For muons the results are of course the same.

The unlike two lepton channel (1.3) only gives a contribution of $2 \times \left(\frac{1}{9}\right) \times \left(\frac{1}{9}\right)$ (not taking tau leptons into account). The remainder consists of more difficult final states involving tau leptons, electron-positron or muon-antimuon pairs.

The two lepton signal has the clear advantage of a low background. It has been discussed in detail in ref. [9]. However, due to the presence of two neutrinos, it is not possible to reconstruct the top mass. For a top search in this signal one has to rely on the event rates and compare them directly with the theoretically calculated $t\bar{t}$ cross section. This results in a top mass with a theoretical error which is not known. These theoretical uncertainties are discussed in detail in section 2. The usefulness of the signal will increase when accompanying jets are measured, but it will become clear that for the discovery of the top quark the study of the 1 lepton signature besides the 2 lepton signature is crucial.

The outline of the paper is as follows. In section 2 the production cross sections and their uncertainties are discussed. In section 3 some methods to determine the top mass which are not sensitive to the absolute value of the cross sections are proposed. Section 4 presents the conclusions.

2 The production cross section and backgrounds

With the use of theoretical calculations the most important consideration is the expected uncertainty in the answer due to the fixed order perturbative calculation. For the top production both signal and background have their uncertainties which affect the applicability of the calculation. In general the correlations between the final state jets and leptons are already predicted well by leading order calculations provided one uses the usual jet definitions. However the normalization of the cross sections is uncertain due to the choice we have to make for the renormalization and factorization scales. One chooses the value of this scale close to the natural scale in the problem in order to minimize the uncalculated higher order contributions. For top production this scale is around the top mass, for the background the scale is around the W mass.

In order to see the sensitivity to the renormalization scale μ which is a measure for the theoretical uncertainty due to the fixed order calculation we make three choices

1. M_W, $\mathrm{m_{top}}$ respectively
2. $\frac{1}{2}M_W$, $\frac{1}{2}\mathrm{m_{top}}$
3. $2\sqrt{M_W^2 + p_{T,W}^2}$, $2\sqrt{\mathrm{m_{top}}^2 + p_{T,t}^2}$

where $p_{T,W}$ is the transverse momentum of the W and $p_{T,t}$ is the average of the transverse momenta of the two tops. The results are given in fig. 1 for the single lepton plus jet final state. The solid lines correspond with the first scale choice, the dashed lines with the second (upper) and third (lower line). Both signal and background are leading order estimates of the cross section. The jet definitions and kinematical cuts used are given in table 1. Note that only by demanding besides the

lepton four jets in the final state the signal and background are comparable up to a top mass of around 150 GeV.

The normalization uncertainty in the background is relatively unimportant when we use distributions. However in the two lepton signal the ability to predict the theoretical cross section as a function of the top mass is crucial. From fig. 2 it is clear that using the leading order prediction for

$$p\bar{p} \rightarrow t\bar{t} \tag{2.1}$$

has a large uncertainty and would make it virtually impossible to determine the top mass using the two lepton signal which relies on the total cross section. However for process (2.1) also the next-to-leading order contributions have been calculated [10]. The next-to-leading order cross section has a reduced sensitivity to the renormalization/factorization scale choices. This is demonstrated in fig. 3 where we show the scale choice sensitivity with the same choices as in leading order. For comparison we also plotted the leading order result with the same choices. One could now in principle use the next-to-leading order calculation with its much smaller theoretical uncertainty to relate the value of the cross section to the top mass. However, in view of the large corrections to the Born cross sections, which amount to about 30 %, one should worry about even higher order contributions. The latter can be approximated by calculating the soft gluon corrections, which has been done in the literature [11]. If we apply this technique to approximate the next-to-leading order contribution we recover the exact next-to-leading order result within about 10% (see fig. 4), well within the theoretical uncertainty. Now we can apply the soft gluon approximation to obtain an estimate of the next-to-next-to-leading order contribution, this gives still a large positive correction of 25 %. The results are summarized in fig. 5, from which it is clear that the estimate of the theoretical uncertainty by changing the scale is not a good method for this particular cross section due to the large corrections. In fact, in ref. [11] the soft gluon effects are calculated to all orders in α_S. For the $q\bar{q}$ subprocess the resummed cross section is about the same size as the $\mathcal{O}(\alpha_S^2)$ corrected cross section, but for the gg subprocess the higher order corrections are large and not well under control.

There are two other uncertainties affecting the top cross section. One results from the parton distribution functions, especially the gluon distribution function. The fraction of the $t\bar{t}$ production that arises from gluon fusion ranges from about 50% for m_{top} = 100 GeV, through 28% for m_{top} = 140 GeV to about 14% for m_{top} = 190 GeV. To show the effect this has, we calculated the cross sections for (2.1) using two different sets of structure functions, see fig. 6. The two sets of structure functions used are the MRSB structure functions [12] with $\Lambda_4 = 122$ MeV and the B1 set of structure functions for the $\overline{MS}$ scheme in [13] with $\Lambda_4 = 126$ MeV. The other uncertainty is a non-perturbative effect resulting from the Coulomb singularity. Its effect on the total cross section is less than 10%. [14]

All the above effects give the predicted next-to-leading order cross section a relatively large uncertainty. Therefore, the top mass determination through the two lepton final state, which relies on the ability to predict the cross section as a function of the top mass, has a larger uncertainty than one might expect through simple renor-

$\sqrt{s}$	1800 GeV
Structure Function	MRSB
Jet rapidity coverage	2
Leptonic rapidity coverage	2
$E_t^{min}(jet)$	15 GeV
$E_t^{min}(lepton)$	20 GeV
$E_t^{min}(missing)$	20 GeV
Jet-Jet separation ΔR	0.7
Jet-lepton separation	none

Table 1. The parameters and cuts used for the one lepton signal and background. For the two lepton signal and background the same parameters and cuts are used. except that no cut is imposed on the missing momentum.

malization scale changes. Since the present CDF limit on m_{top} is based on a next-to-leading order calculation which gives a cross section of 156 pb for $m_{top} = 91$ GeV, use of a next-to-next-to-leading order cross section could possibly increase the m_{top} limit to 95 GeV. This is based on the value of the $\mathcal{O}(\alpha_S^2)$ corrected cross section of 155 pb at $m_{top} = 95$ GeV. This clearly demonstrates the strong sensitivity to radiative effects of the resulting top mass determination.

3 Determination of the top mass

As we have shown in the previous section there will be problems when one relies on the absolute theoretical prediction of the signal to determine the top mass. Therefore we will explore in this section a few possible methods of circumventing these uncertainties.

The first method uses the fact that signal can have various numbers of jets in the final state. Differentiating between these jet final states enables us to form ratios of cross sections with different number of jets. In the approximation that the top is produced on shell the production cross section (2.1) factorizes with respect to the subsequent decay of the top and cancels in the ratio, thus the uncertainties in the production process are removed. Because the energy of the b quark is strongly related to the top mass there will be a strong dependence in the jet fractions and ratios on the top mass. The jet definitions and other kinematical cuts used are listed in table 1.

However this way to cancel the normalization uncertainty in the top cross section only works when the background is negligible. This means the method can only be applied to the two lepton signal and not to the single lepton plus multijets signal. By measuring the 0, 1 or 2 jets arising from energetic b quarks in the top pair decay, we can define jet fractions f_0, f_1 and f_2 by

$$f_i = \frac{\sigma_i}{\sigma_0 + \sigma_1 + \sigma_2} \tag{3.1}$$

where σ_i is the cross section for $p\bar{p} \rightarrow$ 2 leptons + i jets. As can be seen from fig. 7 these fractions have a marked top mass dependence, while there is almost no dependence on the scale. A measurement of such fractions gives an indication of the top mass without relying on the absolute event rates.

If one wants to use a jet fraction method in the single lepton plus jets channel the background has to be reduced to a negligible contribution. This in fact can be accomplished by b tagging for the 3 and 4 jets signal. It reduces the background by a factor of 50 for 3 jets and 30 for 4 jets while leaving the top cross section virtually unaffected. Thus the ratio of the 3 and 4 jets rates again is a useful tool.

The single lepton plus multijets final state offers a more direct possibility of determining the top mass. This is because the top mass is reconstructible from the final state using distributions. Possible uncertainties in the event rates are relatively unimportant provided that the signal to background ratio is of order unity. In ref. [15] several distributions were examined in the lepton plus three jet final state. However the lepton plus four jet final state offers a better possibility since the signal to background ratio is expected to be much more favorable (see fig. 1).

In order to extract the top mass from the signal we will use two simple directly measurable quantities, the three jet invariant mass and the cluster mass. Using the momentum of one of the four jets, the momentum of the charged lepton and the missing transverse momentum, the cluster mass is defined as:

$$m_c(j,l;\nu)^2 = \left[p_T^0(jl) + p_T(\nu)\right]^2 - \left[\mathbf{p}_T(jl) + \mathbf{p}_T(\nu)\right]^2 \tag{3.2}$$

where

$$p_T^0(jl) = \sqrt{\mathbf{p}_T(jl)^2 + m(jl)^2}, \tag{3.3}$$

$$\mathbf{p}_T(jl) = \mathbf{p}_T(j) + \mathbf{p}_T(l), \tag{3.4}$$

$$m(jl)^2 = \left[E(j) + E(l)\right]^2 - \left[\mathbf{p}(j) + \mathbf{p}(l)\right]^2. \tag{3.5}$$

The 3 jet mass is defined using the momenta of three of the four jets:

$$m(j_1,j_2,j_3) = \sqrt{\left[E(j_1) + E(j_2) + E(j_3)\right]^2 - \left[\mathbf{p}(j_1) + \mathbf{p}(j_2) + \mathbf{p}(j_3)\right]^2}. \tag{3.6}$$

All the following calculations are performed with scale 1. The results refer to the sum of the e^+ and e^- signals. In fig. 8 the average cluster mass distributions (one entry for each of the four possible cluster masses) are shown due to signal and background. The histogram due to background alone is indicated with a dashed line. Four top mass cases are presented: 105, 135, 165 and 195 GeV. For the latter two cases the top mass is not visible anymore, for the others a sharp drop indicates the top mass position.

A better signal is obtained by using the the 3 jet mass distributions which are shown in fig. 9 for both signal and background. Again the background contribution is given by the dashed histogram. Above a top mass of 165 GeV the top signal is too small with respect to the background, making the peak virtually invisible.

We can easily improve these invariant mass distributions by using more of the kinematics of the top events. The cluster masses and the three jet masses can be

grouped into pairs, each consisting of a cluster mass calculated from one jet momentum and a three jet mass calculated from the three *other* momenta. By selecting the pair in each event, in which the cluster mass and the three jet mass are closest in value, two additional distributions are obtained. Each event gives one entry in a cluster mass histogram and one in a three jet mass histogram. The signals improve dramatically in these distributions. This can be seen in figs. 10 and 11.

With this algorithm we also studied other top mass values. Up to 160 GeV the top signal remains clearly visible, especially in the constrained three jet mass (fig. 11). Of course no experimental detector effects are taken into account. The shown distributions would be the result when one uses the true jets and leptons, not affected by the detector acceptance. Determination of the top mass using these invariant masses is straightforward and direct leaving no doubt whether or not there is a top or what its mass is.

4 Conclusions

In this paper we have shown that the one lepton plus 4 jets channel is crucial for establishing the top quark. With this signal it becomes possible to study distributions where the top reveals itself by a clear peak at the top mass. Of course the experimental resolution will modify the shapes, but a priori the signal shows up above the background. The advantage of this method is that the top mass determination is straightforward, making analysis of the theoretical and experimental uncertainties simple. Of course the use of a distribution makes it necessary to require a reasonable number of events. With an integrated luminosity of 25 pb^{-1} one can expect of the order of 50 events in this channel for a top mass around 135 GeV making this method applicable.

References

[1] F. Abe et al., Phys. Rev. Lett. **68** (1992) 447.

[2] The LEP collaborations: ALEPH, DELPHI, L3 and OPAL, Phys. Lett. **B276** (1992) 247.

[3] R.K. Ellis and S. Parke, "Top quark production by W-gluon fusion", Fermilab-Pub-92/132-T.

[4] Z. Kunszt and W.J. Stirling, Phys. Rev. **D37** (1988) 2439.

[5] W.T. Giele, D.A. Kosower and H. Kuijf, Nucl. Phys. **B** (Proc. Suppl.) **23B** (1991) 22.

[6] F.A. Berends, H. Kuijf, B. Tausk and W.T. Giele, Nucl. Phys. **B357** (1991) 32.

[7] K. Hagiwara and D. Zeppenfeld, Nucl. Phys. **B313** (1989) 560.

[8] F.A. Berends, W.T. Giele and H. Kuijf, Nucl. Phys. **B321** (1989) 39.

[9] H. Baer, V. Barger and R.J.N. Phillips, Phys. Rev. **D39** (1989) 3310.

[10] P. Nason, S. Dawson and R.K. Ellis, Nucl. Phys. **B303** (1988) 607;
W. Beenakker, H. Kuijf, W.L. van Neerven and J. Smith, Phys. Rev. **D40** (1989) 54.

[11] E. Laenen, J. Smith and W.L. van Neerven, Nucl. Phys. **B369** (1992) 543.

[12] A.D. Martin, R.G. Roberts and W.J. Stirling, Phys. Lett. **B206** (1988) 327.

[13] J.G. Morfín and W.K. Tung, Z. Phys. **C52** (1991) 13.

[14] V. Fadin, V. Khoze and T. Sjöstrand, Z. Phys. **C48** (1990) 613.

[15] W.T. Giele and W.J. Stirling, Nucl. Phys. **B343** (1990) 14.

Fig. 1. a,b and c: The cross sections for $p\bar{p} \rightarrow$ lepton + 2,3, and 4 jets, respectively. The curves show the $t\bar{t}$ signal, the horizontal lines are the QCD background. Fig. 1d shows the total $p\bar{p} \rightarrow$ lepton + jets cross section.

Fig. 2. The Born approximation to the total $p\bar{p} \rightarrow t\bar{t}$ cross section using the MRSB structure functions for several choices of the renormalization scale μ.

Fig. 3. Solid lines: the next-to-leading order $p\bar{p} \rightarrow t\bar{t}$ cross section using the MRSB structure functions. Dashed lines: the Born cross section.

Fig. 4. A comparison of the exact next-to-leading order $p\bar{p} \rightarrow t\bar{t}$ cross section and the soft gluon approximation using the MRSB structure functions.

Fig. 5. The total $p\bar{p} \rightarrow t\bar{t}$ cross section using the MRSB structure functions. The top curve includes the $\mathcal{O}(\alpha_S^2)$ contribution in the soft gluon approximation; the other curves are the exact $\mathcal{O}(\alpha_S)$ corrected cross sections for three choices of the scale μ.

Fig. 6. The total $\mathcal{O}(\alpha_S)$ corrected $p\bar{p} \rightarrow t\bar{t}$ cross section using two different sets of structure functions.

Fig. 7. The fractions of all $p\bar{p} \rightarrow t\bar{t} \rightarrow$ 2 leptons + jets events with 0, 1 and 2 jets.

Fig. 8. Cluster mass distributions for four values of m_{top}. The solid lines show the signal plus the background; the dotted lines show the background contribution.

Fig. 9. Three-jet-mass distributions for four values of m_{top}. The solid lines show the signal plus the background; the dotted lines show the background contribution.

Fig. 10. The distribution of the cluster mass belonging to the selected pair for four values of m_{top}. The solid lines show the signal plus the background; the dotted lines show the background contribution.

Fig. 11. The distribution of the three-jet-mass belonging to the selected pair for four values of m_{top}. The solid lines show the signal plus the background; the dotted lines show the background contribution.

Figure 1

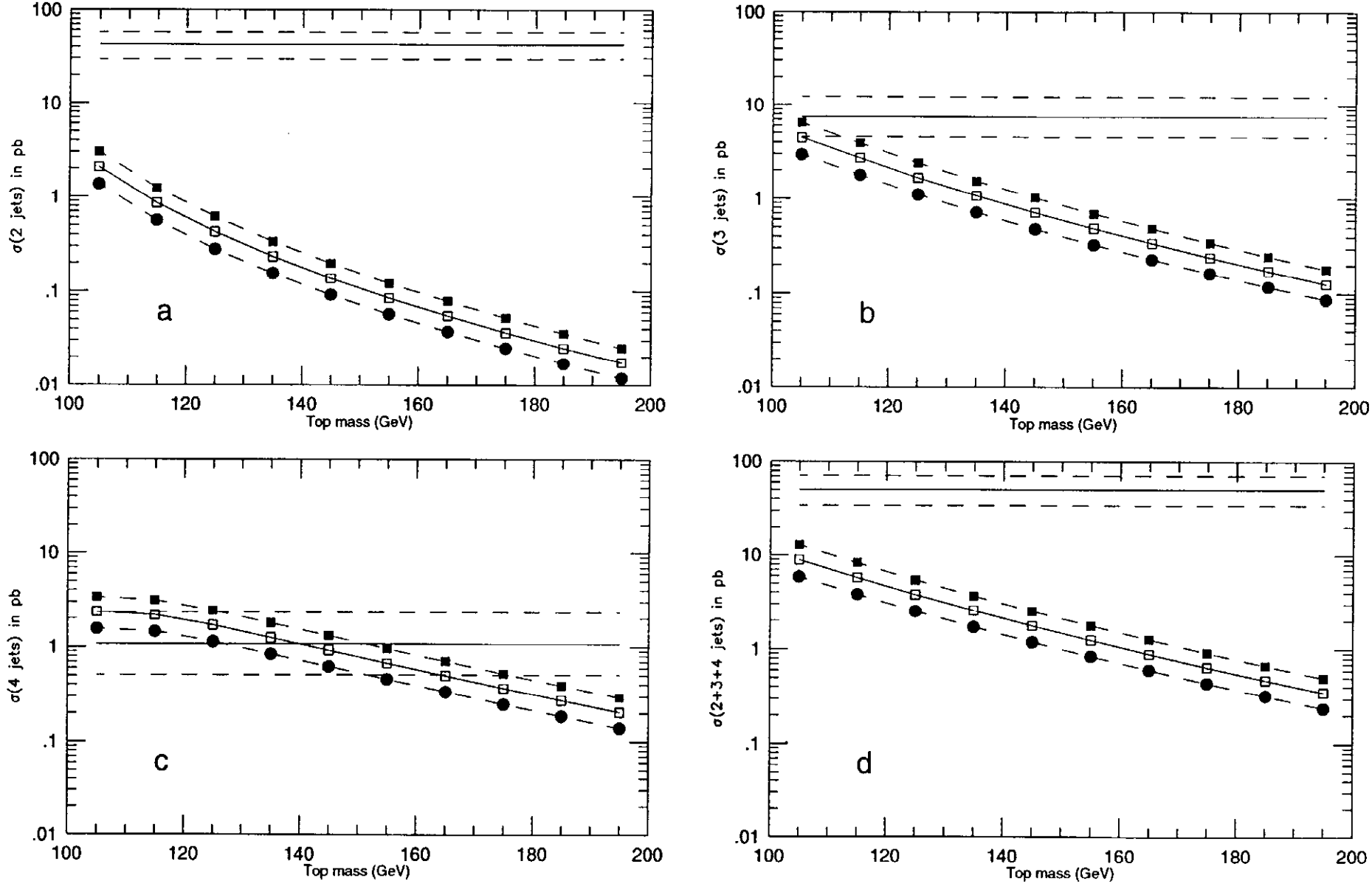
100
10
1
.1
.01
σ(2 jets) in pb
a
100
120
140
160
180
200
Top mass (GeV)
σ(3 jets) in pb
b
σ(4 jets) in pb
c
σ(2+3+4 jets) in pb
d

Figure 2

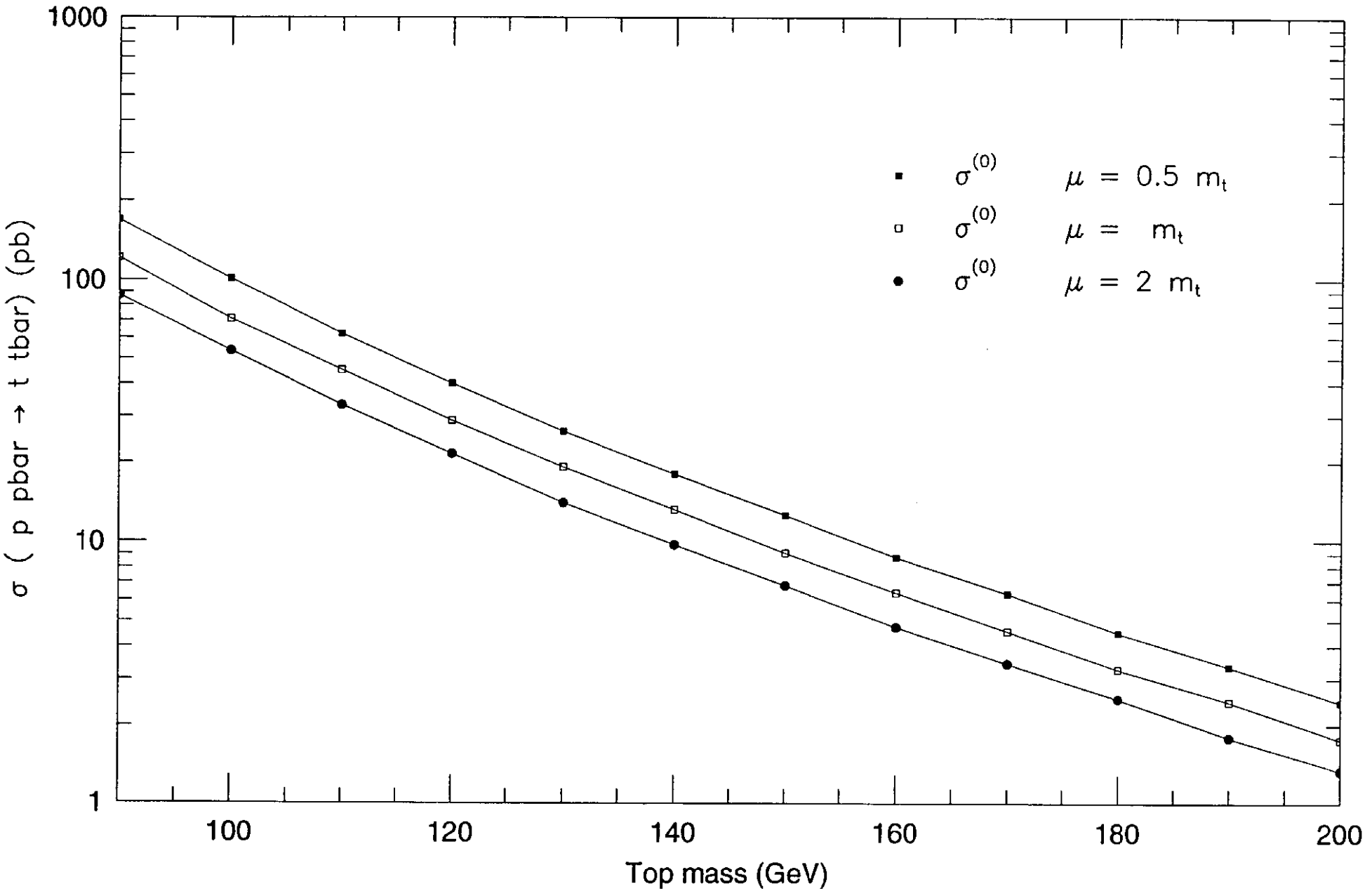
1000
100
10
1
σ (p pbar → t tbar) (pb)
100
120
140
160
180
200
Top mass (GeV)
σ(0) μ = 0.5 mt
σ(0) μ = mt
σ(0) μ = 2 mt

Figure 3

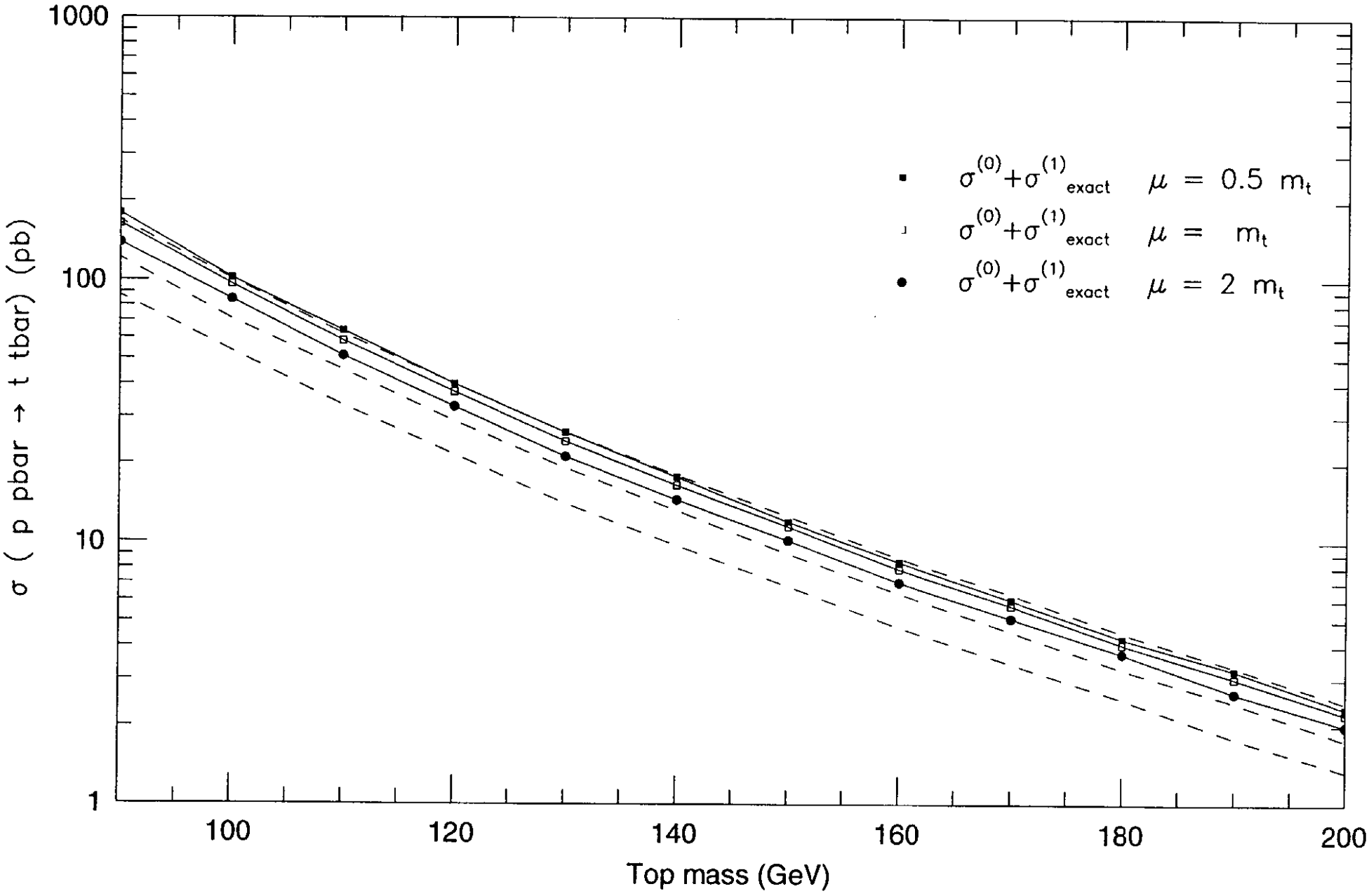
1000
100
10
1
σ (p pbar → t tbar) (pb)
100
120
140
160
180
200
Top mass (GeV)
σ(0)+σ(1) exact μ = 0.5 mt
σ(0)+σ(1) exact μ = mt
σ(0)+σ(1) exact μ = 2 mt

Figure 4

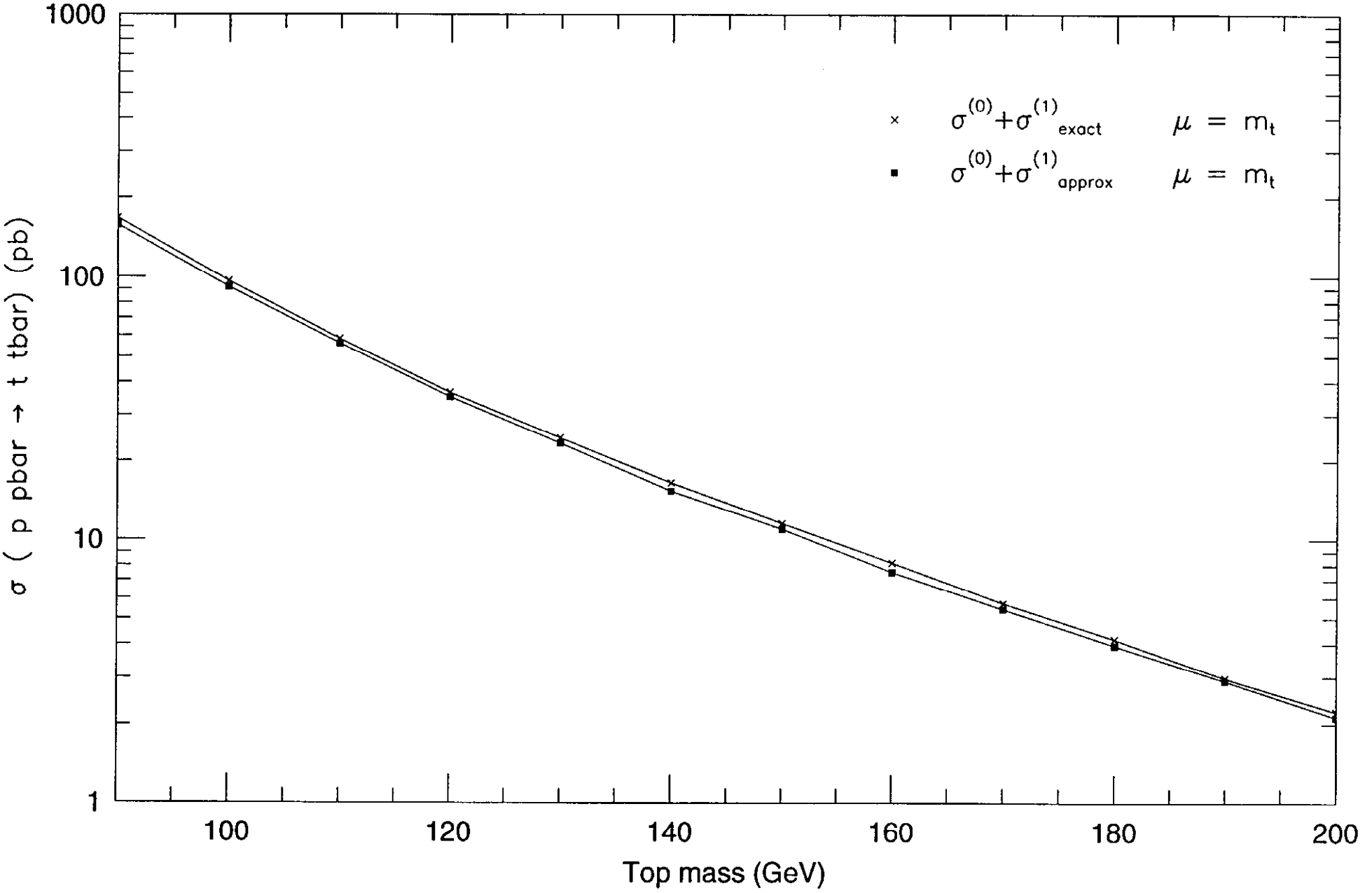
1000
100
10
1
σ (p pbar → t tbar) (pb)
100
120
140
160
180
200
Top mass (GeV)
× σ(0)+σ(1) exact μ = mt
■ σ(0)+σ(1) approx μ = mt

Figure 5

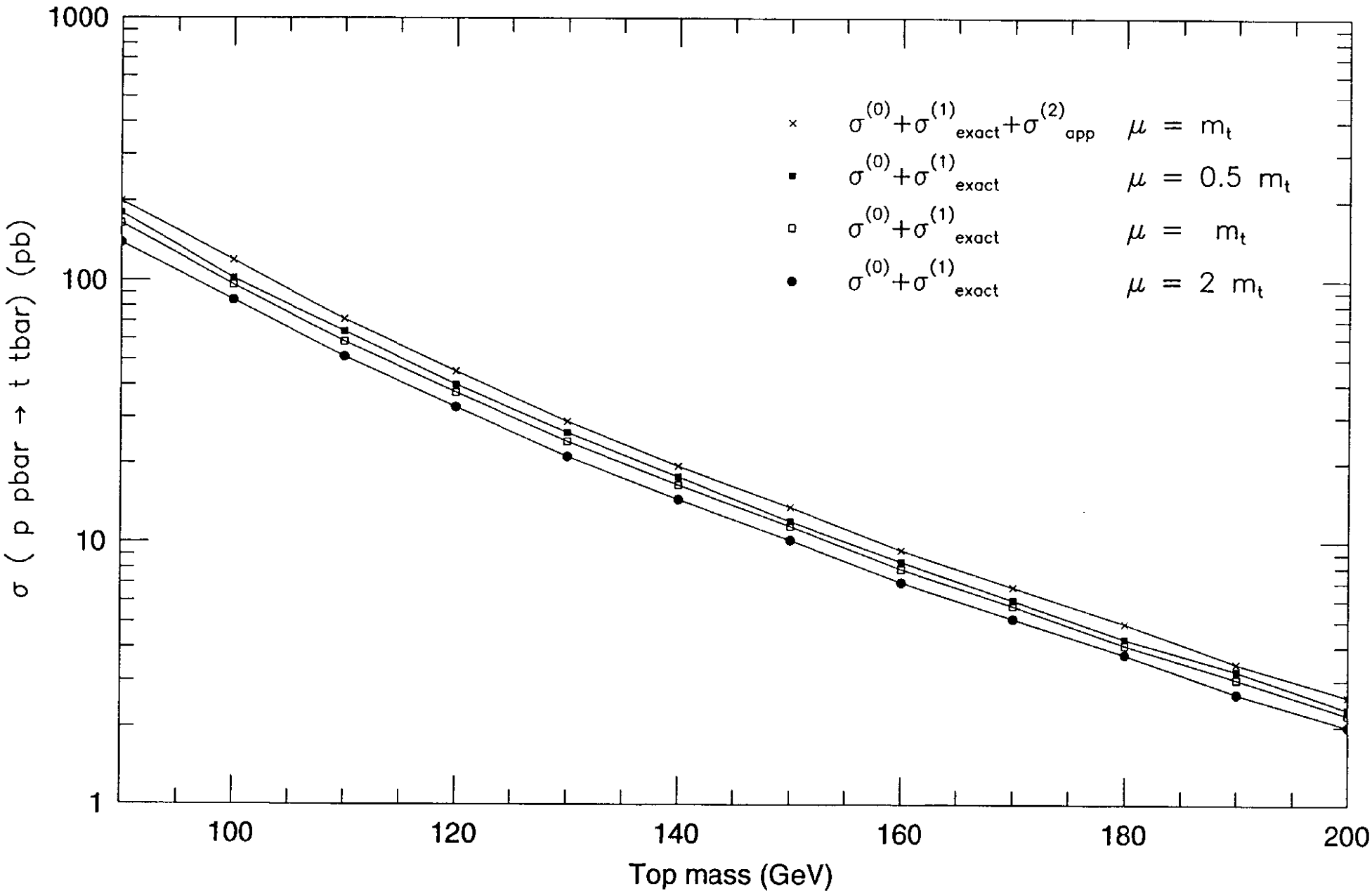
1000
100
10
1
σ (p pbar → t tbar) (pb)
100
120
140
160
180
200
Top mass (GeV)
σ(0)+σ(1)exact+σ(2)app μ = mt
σ(0)+σ(1)exact μ = 0.5 mt
σ(0)+σ(1)exact μ = mt
σ(0)+σ(1)exact μ = 2 mt

Figure 6

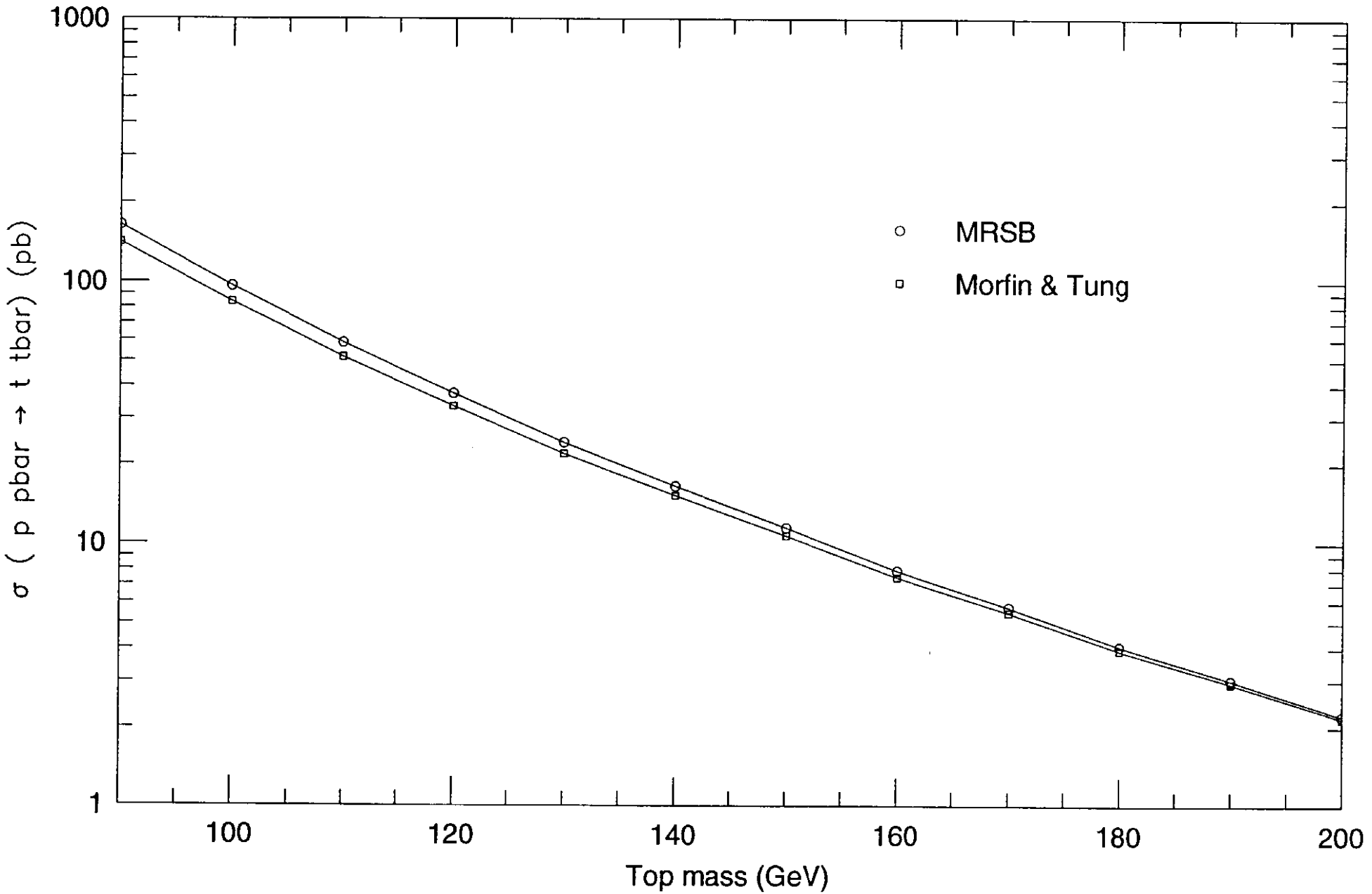
1000
100
10
1
σ (p pbar → t tbar) (pb)
MRSB
Morfin & Tung
100
120
140
160
180
200
Top mass (GeV)

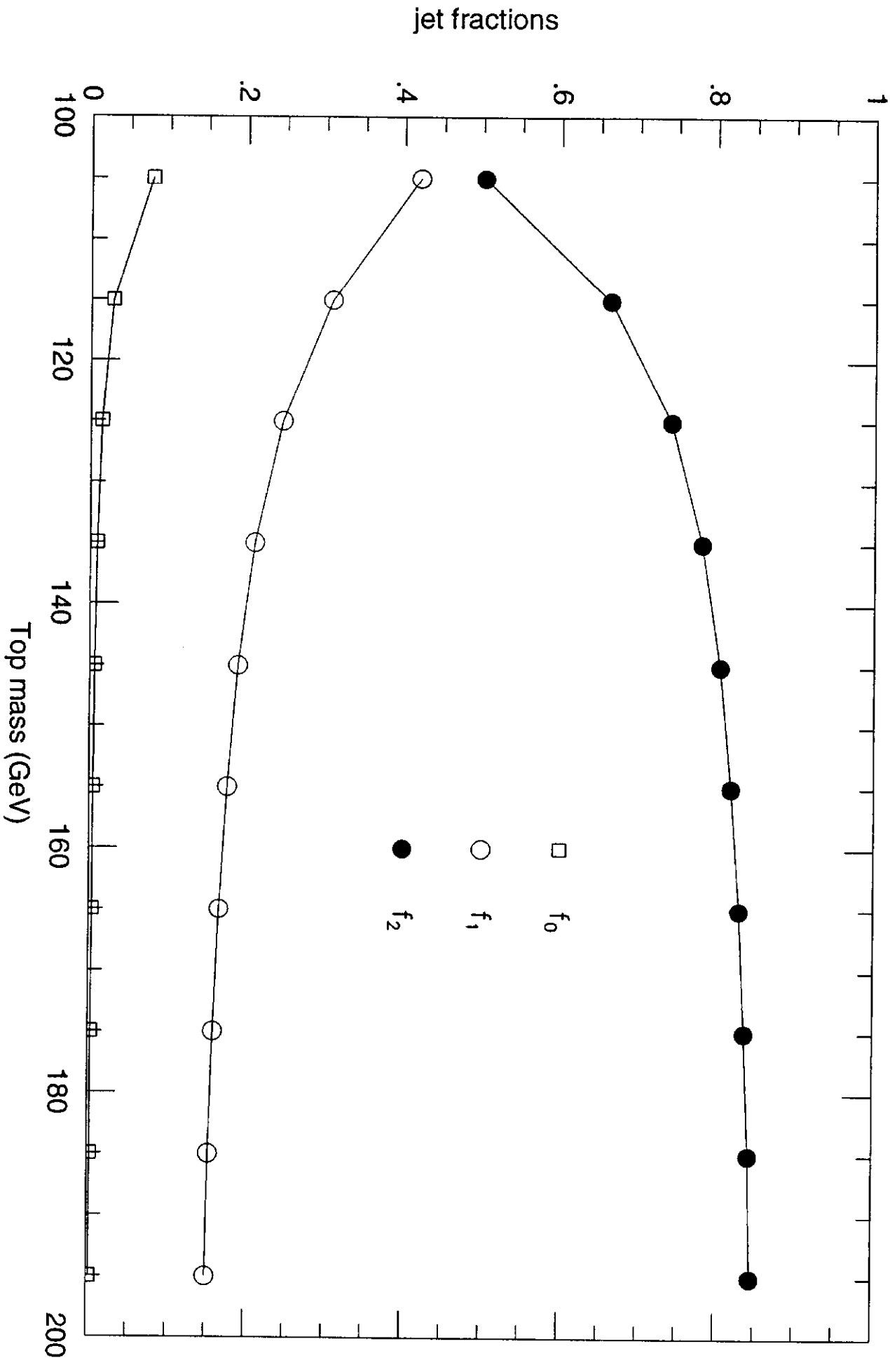
jet fractions
0
.2
.4
.6
.8
1
100
120
140
160
180
200
Top mass (GeV)
f_0
f_1
f_2

Figure 7

Figure 8

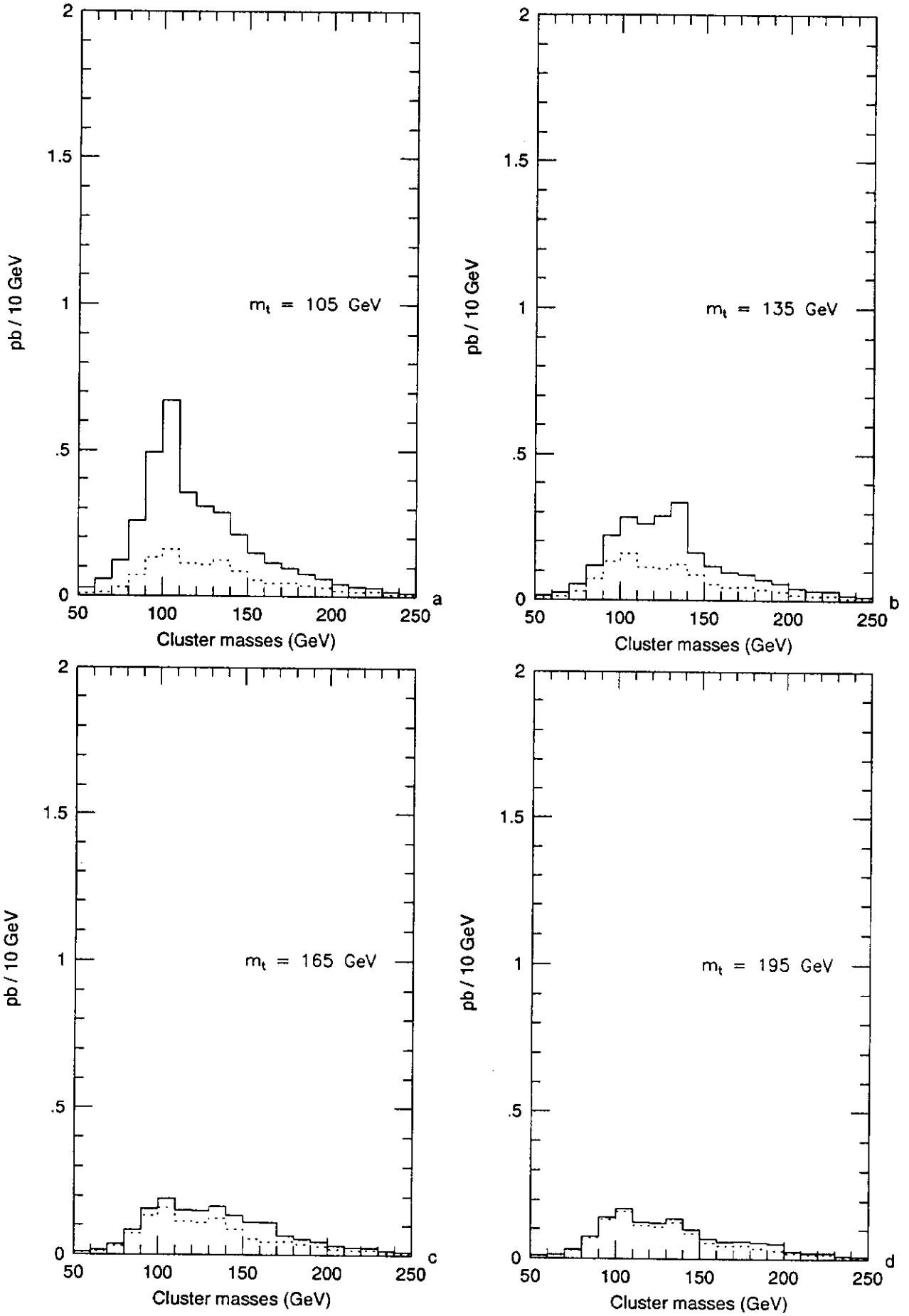
pb / 10 GeV
m_t = 105 GeV
a
Cluster masses (GeV)
pb / 10 GeV
m_t = 135 GeV
b
Cluster masses (GeV)
pb / 10 GeV
m_t = 165 GeV
c
Cluster masses (GeV)
pb / 10 GeV
m_t = 195 GeV
d
Cluster masses (GeV)

Figure 9

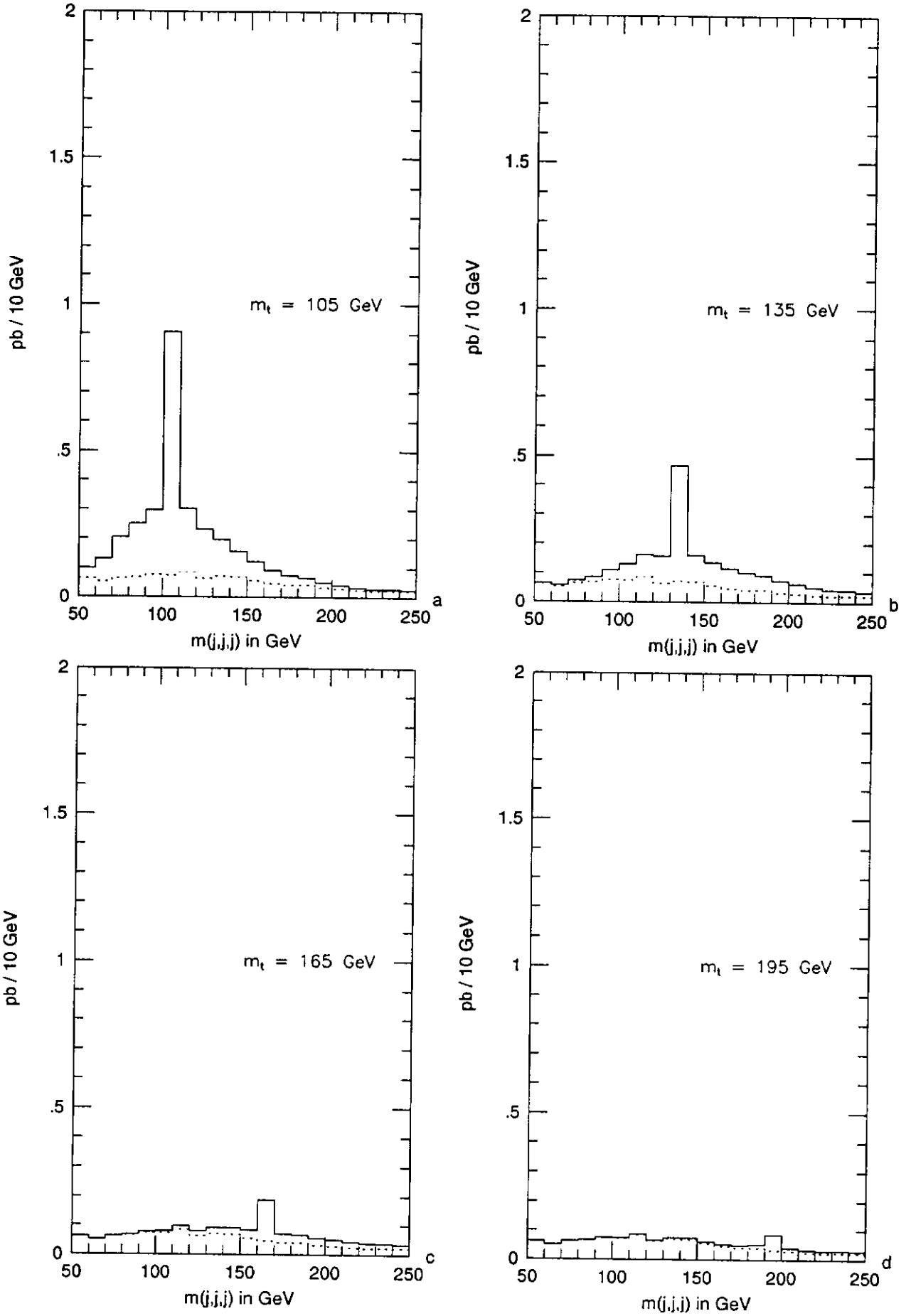
pb / 10 GeV
m(j,j,j) in GeV
m_t = 105 GeV
a
m_t = 135 GeV
b
m_t = 165 GeV
c
m_t = 195 GeV
d

Figure 10

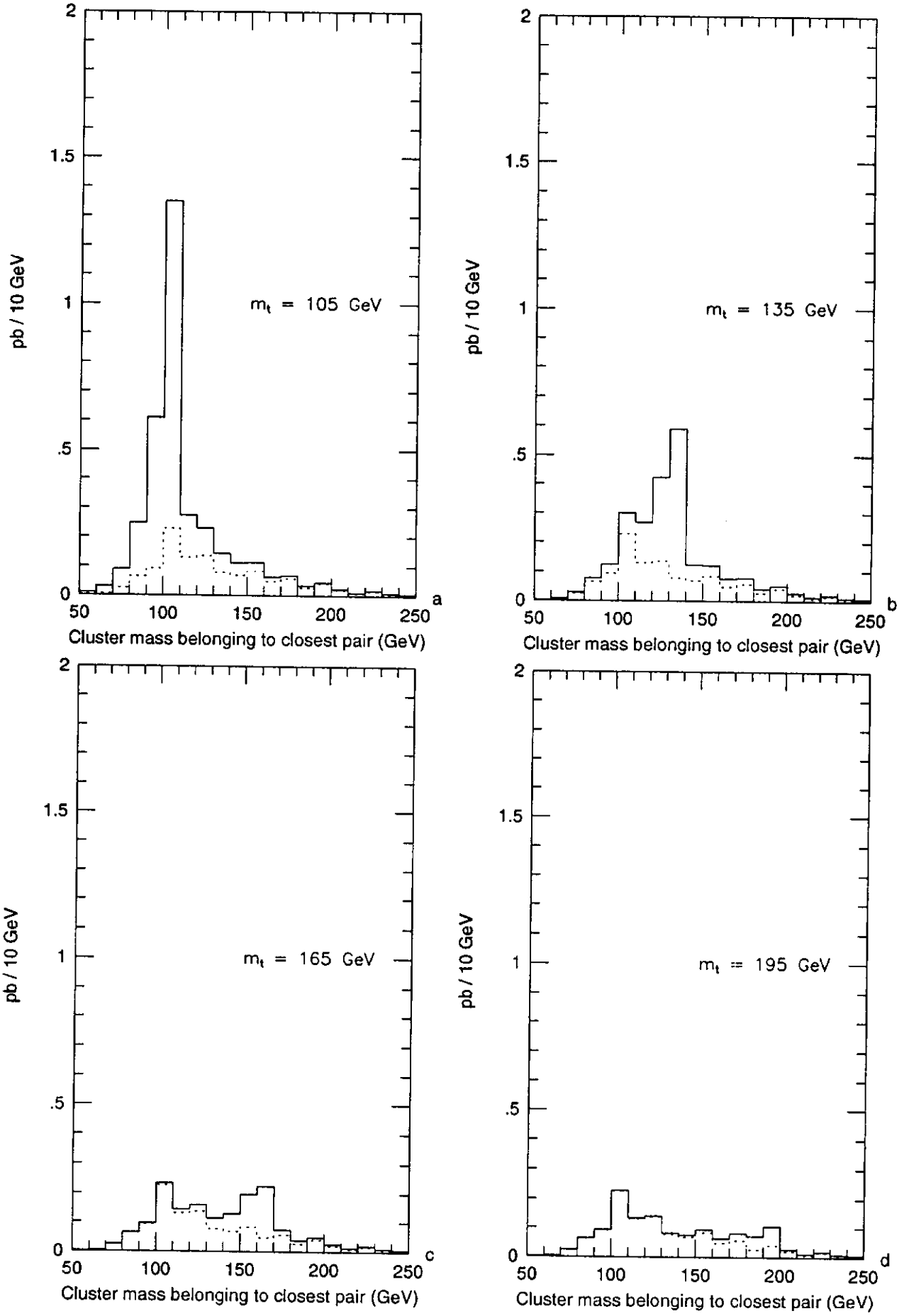
pb / 10 GeV
m_t = 105 GeV
a
Cluster mass belonging to closest pair (GeV)
pb / 10 GeV
m_t = 135 GeV
b
Cluster mass belonging to closest pair (GeV)
pb / 10 GeV
m_t = 165 GeV
c
Cluster mass belonging to closest pair (GeV)
pb / 10 GeV
m_t = 195 GeV
d
Cluster mass belonging to closest pair (GeV)

Figure 11

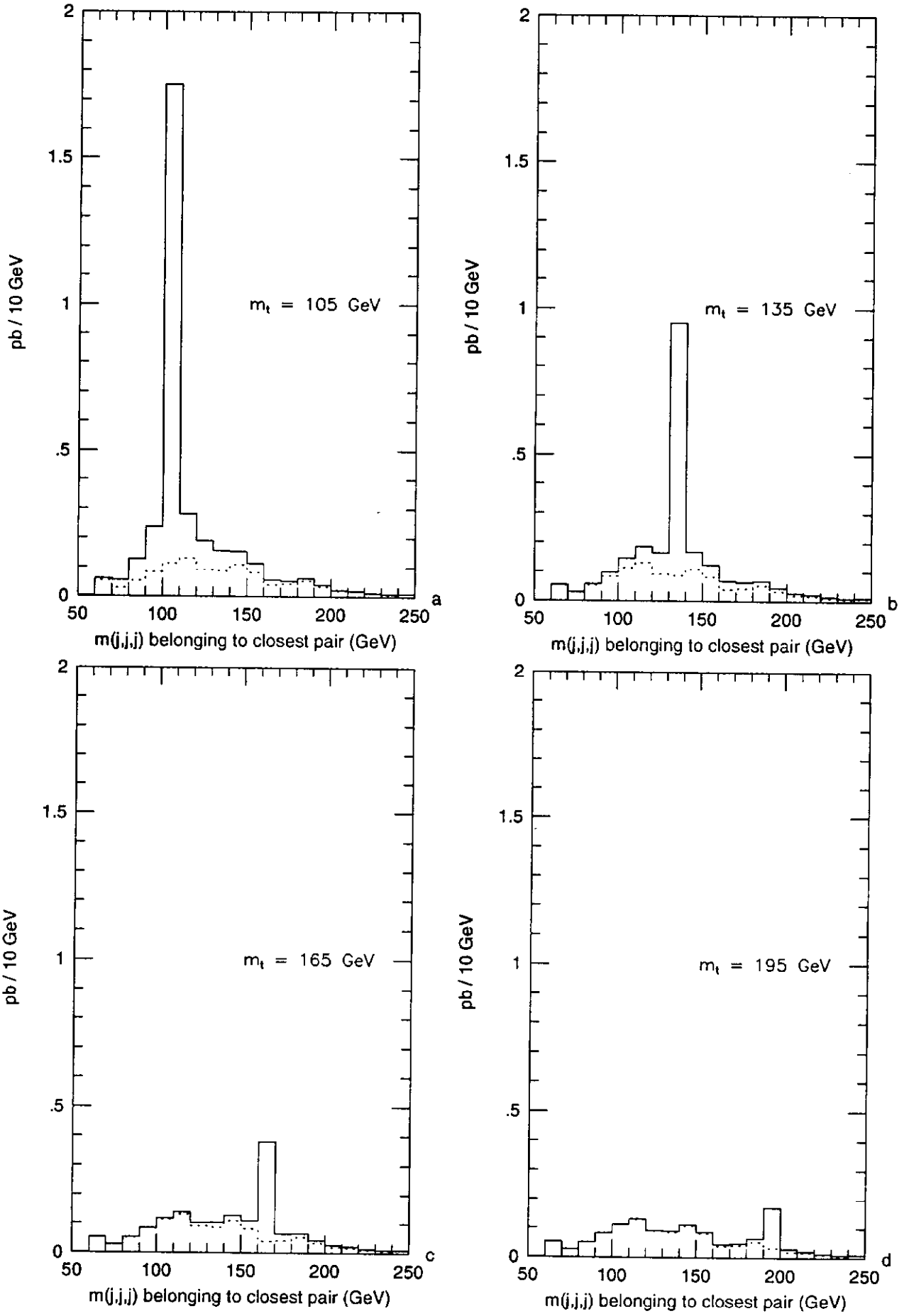
pb / 10 GeV
m(j,j,j) belonging to closest pair (GeV)
m_t = 105 GeV
a
m_t = 135 GeV
b
m_t = 165 GeV
c
m_t = 195 GeV
d